

# Pt-Containing Ag<sub>2</sub>S-Noble Metal Nanocomposites as Highly Active Electrocatalysts for the Oxidation of Formic Acid

Hui Liu<sup>1,2</sup>, Yan Feng<sup>1,2</sup>, Hongbin Cao<sup>3,\*</sup>, Jun Yang<sup>1,\*</sup>

(Received 24 January 2014; accepted 10 March 2014; published online July 1, 2014)

**Abstract:** Nanocomposites with synergistic effect are of great interest for their enhanced properties in a given application. Herein, we reported the high catalytic activity of Pt-containing Ag<sub>2</sub>S-noble metal nanocomposites in formic acid oxidation, which is a key reaction in direct formic acid fuel cell. The electrochemical measurements including voltammograms and chronoamperograms are used to characterize the catalytic property of Pt-containing nanocomposites for the oxidation of formic acid. In view of the limited literatures on using nanocomposites consisting of semiconductor and noble metals for catalyzing the reactions of polymer electrolyte membrane-based fuel cells, this study provides a helpful exploration for expanding the application of semiconductor-noble metal nanocomposites.

**Keywords:** Nanocomposites; Synergistic effect; Formic acid oxidation; Direct formic acid fuel cell

**Citation:** Hui Liu, Yan Feng, Hongbin Cao and Jun Yang, "Pt-Containing Ag<sub>2</sub>S-Noble Metal Nanocomposites as Highly Active Electrocatalysts for the Oxidation of Formic Acid", *Nano-Micro Lett.* 6(3), 252-257 (2014). <http://dx.doi.org/10.5101/nml140027a>

## Introduction

Platinum (Pt) nanoparticles are active electrocatalysts to facilitate both anodic and cathodic reactions in polymer electrolyte membrane fuel cells (PEMFCs) [1-3]. However, in methanol or formic acid-fed PEMFCs, the Pt catalysts usually suffer from the poisoning at the anode by carbon monoxide (CO), which is an intermediate product of the fuels [4-7]. Over the past few decades, a number of strategies including the reduction of particle size, taking control of particle shape and structure, and alloying with transitional metals [3,8-12], have been successfully used to enhance the Pt electrocatalytic activity and resistance to deactivation.

Our recent work demonstrated that the integration of Pt with a suitable semiconductor might be an effective way to improve the catalytic property of Pt for PEMFC

reactions [13,14]. For example, in the Ag<sub>2</sub>S-noble metal nanomaterials reports recently, the Pt-containing nanocomposites were found to display excellent catalytic activity for methanol oxidation, due to electron donation from the semiconductor domains to the ultrafine Pt crystallites [13]. In addition, in core-shell structured CdSe-Pt nanocomposites were obtained by reducing platinum precursors by sodium citrate in the presence of previously formed CdSe nanocrystals, and the compressive strain effect imposed from the CdSe core on the deposited Pt shell results in an appropriate downshift of the d band center of Pt catalysts, which leads to the enhancement of the core-shell structured nanocomposites for catalyzing the oxygen reduction and methanol oxidation in direct methanol fuel cells [14].

Herein, we reported our experimental extensions on

<sup>1</sup>State Key Laboratory of Multiphase Complex Systems, Institute of Process Engineering, Chinese Academy of Sciences, Beijing 100190, China

<sup>2</sup>University of Chinese Academy of Sciences, No. 19A Yuquan Road, Beijing 100049, China

<sup>3</sup>Research Centre for Process Pollution Control, Institute of Process Engineering, Chinese Academy of Sciences, Beijing 100190, China

\*Corresponding author. E-mail: [jyang@mail.ipe.ac.cn](mailto:jyang@mail.ipe.ac.cn); [hbcdo@mail.ipe.ac.cn](mailto:hbcdo@mail.ipe.ac.cn)

the formic acid oxidation reaction (FAOR) using Pt-containing Ag<sub>2</sub>S-noble metal nanocomposites as electrocatalysts. Oxidation of Formic acid is a key reaction of direct formic acid fuel cell (DFAFC) [15,16], in which the low crossover rate of formic acid through the Nafion membrane allows higher fuel concentrations to be used than in the case of direct methanol fuel cell (DMFC) [17]. In view of the quite limited literatures on using nanocomposites consisting of semiconductor and noble metals for PEMFC reactions, this study might be a salutary exploration for expanding the application of semiconductor-metal nanocomposites.

## Experimental sections

### Materials

The reagents, if not indicated specifically, were from Sigma-Aldrich; ethanol, and toluene were from Beijing Chemical Works; bis (*p*-sulfonatophenyl) phenylphosphane dihydrate dipotassium salt (BSPP) was from Strem Chemicals; and Vulcan XC-72 carbon powders were from Cabot. All glassware and Teflon-coated magnetic stirring bars were cleaned with aqua regia, followed by copious rinsing with de-ionized water before drying in an oven.

### Synthesis of Ag<sub>2</sub>S nanocrystals and Ag<sub>2</sub>S-noble metal nanocomposites

The syntheses of Ag<sub>2</sub>S nanocrystals and Ag<sub>2</sub>S-noble metal nanocomposites followed a protocol reported previously with modifications [13]. In a typical synthesis of a hydrosol of monoclinic Ag<sub>2</sub>S nanocrystals, 600 mg of BSPP was added to 300 mL of aqueous AgNO<sub>3</sub> solution (1 mM). The mixture was stirred for 1 h, followed by the prompt addition of 10 mL of aqueous Na<sub>2</sub>S solution (50 mM). A brownish hydrosol was obtained after stirring the reaction mixture at room temperature for 4 h, indicating the formation of Ag<sub>2</sub>S nanocrystals.

A more simplified protocol was used to prepare Ag<sub>2</sub>S-Pt and Ag<sub>2</sub>S-Au-Pt nanocomposites. In brief, 60 mL of the Ag<sub>2</sub>S hydrosol was refluxed at 110°C for 3 min in a 100-mL three-necked flask equipped with a condenser and a Teflon-coated magnetic stirring bar. Next, 3 mL of aqueous sodium citrate solution (100 mM) was added. The resulting mixture was refluxed for 1 min at 110°C, and then 1.2 mL of aqueous H<sub>2</sub>PtCl<sub>6</sub> solution (50 mM) or a mixture of 1.2 mL of aqueous HAuCl<sub>4</sub> solution (50 mM) and 1.2 mL of aqueous solution of H<sub>2</sub>PtCl<sub>6</sub> (50 mM) were added swiftly. The reaction mixture was continuously refluxed for 2 h at 110°C to form a hydrosol of Ag<sub>2</sub>S-Pt or Ag<sub>2</sub>S-Au-Pt nanocomposite.

Ag<sub>2</sub>S-Au nanocomposites and pure Pt nanoparticles with analogous size to the Pt domain in the Pt-

containing nanocomposites were also prepared for comparison. For Ag<sub>2</sub>S-Au, 60 mL of the Ag<sub>2</sub>S hydrosol was refluxed at 105°C for 3 min, followed by the addition of 3 mL of aqueous sodium citrate solution (100 mM). The resulting mixture was refluxed for 1 min at 105°C, and then 1.2 mL of aqueous HAuCl<sub>4</sub> solution (50 mM) was added swiftly. The reaction mixture was continuously refluxed for 30 min at 105°C to form a hydrosol of Ag<sub>2</sub>S-Au nanocomposite. The tiny Pt nanoparticles were prepared using an ethanol mediated phase transfer protocol [18]. In a typical experiment, 50 mL of 1 mM of aqueous H<sub>2</sub>PtCl<sub>6</sub> solution was mixed with 50 mL of ethanol containing 1 mL of dodecylamine. After 3 min of stirring, 50 mL of toluene was added, and stirring was continued for more than 1 minute. The Pt precursors in toluene were separated from the aqueous phase, and mixed with 3 mL of aqueous NaBH<sub>4</sub> solution (100 mM). The mixture was agitated for several minutes to form Pt organosol in toluene.

After preparation, the Ag<sub>2</sub>S-noble metal nanocomposites (Ag<sub>2</sub>S-Au, Ag<sub>2</sub>S-Pt, and Ag<sub>2</sub>S-Au-Pt) were also transferred in toluene using the ethanol mediated phase transfer method for the standardization of the particle surface, which is important for further electrochemical comparison. After the phase transfer treatment, the Ag<sub>2</sub>S-noble metal nanocomposites and the monometallic Pt nanoparticles would have the same stabilizer molecules (dodecylamine) adsorbed on their surfaces. In addition, the phase transfer of nanocomposites from aqueous phase to a non-polar organic medium was conducted since we experimentally found that the loading efficiency of the particles on XC-72C carbon powders from the organic medium (~99%) was much higher than that from the aqueous phase (~37%). Typically, the Ag<sub>2</sub>S-metal hydrosol was mixed with an equal volume of ethanolic solution of dodecylamine (90 mM). After 5 min of stirring, an equal volume of toluene was added and stirred for 3 minutes. Phase transfer of the Ag<sub>2</sub>S-metal nanocomposite from water to toluene would then occur quickly and completely, leaving a clear colorless solution in the aqueous phase.

### Particle characterizations

Transmission electron microscopy (TEM) was performed on a JEOL JEM-2100 electron microscope operated at 200 kV with the software package for automated electron tomography. A drop of the nanoparticle solution was first dispensed onto a 3-mm carbon-coated copper grid. Excessive solution was removed by an absorbent paper, and the sample was dried under vacuum at room temperature. An EDX analyzer attached to the TEM was used to analyze the components in samples. XPS analyses were conducted on an ESCALAB MKII spectrometer (VG Scientific) using Al-K<sub>α</sub> radiation (1486.71 eV). Samples for XPS were concentrated

from the toluene solution of Pt nanoparticle or  $\text{Ag}_2\text{S}$ -metal nanocomposite to 0.5 mL using flowing Ar. 10 mL of ethanol was then added to precipitate the particles, which were then recovered by centrifugation, and washed with ethanol several times, and dried at room temperature in vacuum.

### Electrochemical measurements

Electrochemical measurements were carried out in a standard three-electrode cell connected to a Bio-logic VMP3 (with EC-lab software version 9.56) potentiostat. A leak-free Ag/AgCl (saturated with KCl) electrode was used as the reference electrode. The counter electrode was a platinum mesh ( $1 \times 1 \text{ cm}^2$ ) attached to a platinum wire.

For the loading of the Pt-containing nanocomposites on Vulcan XC-72 carbon support, a calculated amount of carbon powder was added to the toluene solution of nanocomposites. After stirring the mixture for 24 h, the nanocomposites/C (20 wt% Pt on carbon support) was collected by centrifugation, and washed thrice with methanol, and then dried at room temperature in vacuum.

The working electrode was a thin layer of Nafion-impregnated catalyst cast on a vitreous carbon disk. This electrode was prepared by ultrasonically dispersing 10 mg of the nanocomposites/C in 10 mL of aqueous solution containing 4 mL of ethanol and 0.1 mL of Nafion. A calculated volume of the ink was dispensed onto the 5 mm glassy carbon disk electrode to produce a nominal catalyst loading of  $20 \mu\text{g cm}^{-2}$  (Pt basis). The carbon electrode was then dried in a stream of warm air at  $70^\circ\text{C}$  for 1 h.

The catalyst performance in room-temperature formic acid oxidation reaction (FAOR) was measured by cyclic voltammetry. For these measurements, the potential window of 0 V to 1 V was scanned at  $20 \text{ mV s}^{-1}$  until a stable response was obtained, before the voltammograms were recorded. The electrolyte was formic acid (1 M) mixed in perchloric acid (0.1 M).

## Results and discussion

### Nanocomposites of $\text{Ag}_2\text{S}$ and noble metals (Au, Pt)

The as-prepared  $\text{Ag}_2\text{S}$  nanocrystals, which were used as seeds for the subsequent deposition of different metals, were shown by the TEM image in Fig. 1(a). The nanocrystals were spherical, nearly monodispersed, and had an average size of 8.4 nm. The high-resolution TEM (HRTEM) image (Fig. 1(b)) illustrated the lattice planes in these nanocrystals, confirming that these  $\text{Ag}_2\text{S}$  particles were of high crystallinity.

As schematically shown in Fig. 2(a) and 2(b), the reduction of metal precursors (Au and Pt) in the presence

of preformed  $\text{Ag}_2\text{S}$  nanocrystals resulted in the heterogeneous deposition of noble metals on the surface of  $\text{Ag}_2\text{S}$ . The obtained nanocomposites were illustrated in Fig. 3(a) and 3(c). The deposition of noble metals on the  $\text{Ag}_2\text{S}$  nanocrystals was clearly identified via brightness contrast, and confirmed by the energy-dispersive X-ray (EDX) analyses (Fig. 3(b) and 3(d)). In addition, Fig. 3(a) and 3(c) illustrated that gold was deposited only at a single site on each  $\text{Ag}_2\text{S}$  nanocrystal, whereas the nucleation and growth of Pt occurred at multiple sites on each  $\text{Ag}_2\text{S}$  nanocrystal.

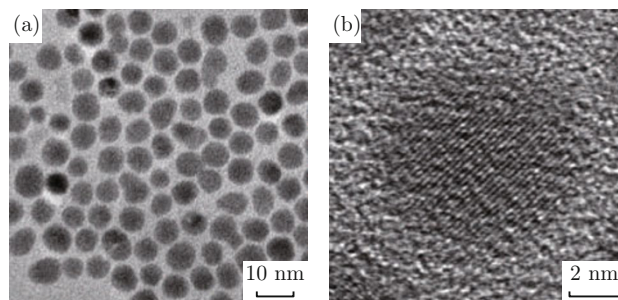


Fig. 1 TEM (a) and HRTEM (b) image of the as-prepared  $\text{Ag}_2\text{S}$  nanocrystals in aqueous phase.

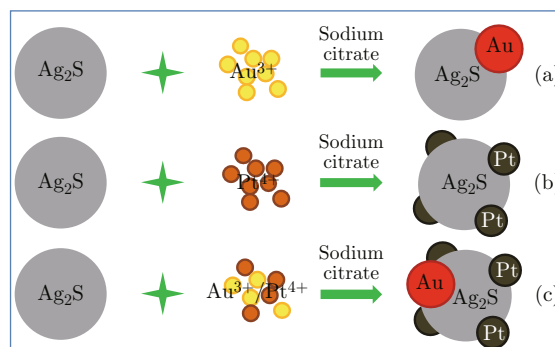


Fig. 2 Schematic illustration to show the heterogeneous deposition of noble metals on the surface of  $\text{Ag}_2\text{S}$  nanocrystals: (a)  $\text{Ag}_2\text{S}$ -Au; (b)  $\text{Ag}_2\text{S}$ -Pt; (c)  $\text{Ag}_2\text{S}$ -Au-Pt.

The different features of Au and Pt deposition on  $\text{Ag}_2\text{S}$  nanocrystal could be further employed to integrate Au, Pt, and  $\text{Ag}_2\text{S}$  into a single nanosystem. Different from the successive synthesis reported previously [13], the ternary  $\text{Ag}_2\text{S}$ -Au-Pt nanocomposites were prepared by co-reduction of  $\text{HAuCl}_4$  and  $\text{H}_2\text{PtCl}_6$  metal precursors using citrate in the presence of preformed  $\text{Ag}_2\text{S}$  nanocrystals (Fig. 2(c)). Fig. 3(e) was the TEM image of the as-prepared  $\text{Ag}_2\text{S}$ -Au-Pt nanocomposites. In comparison with the TEM images of Fig. 3(a) and 3(c), the domains with enhanced contrast and larger particle size ( $\sim 3 \text{ nm}$ ) in the nanocomposites could be indexed to gold, whereas Pt metal in the same nanocomposites appeared as smaller dots ( $\sim 1 \text{ nm}$ ). The presence of Au, Pt, and  $\text{Ag}_2\text{S}$  in the nanocomposite particles was confirmed by the EDX

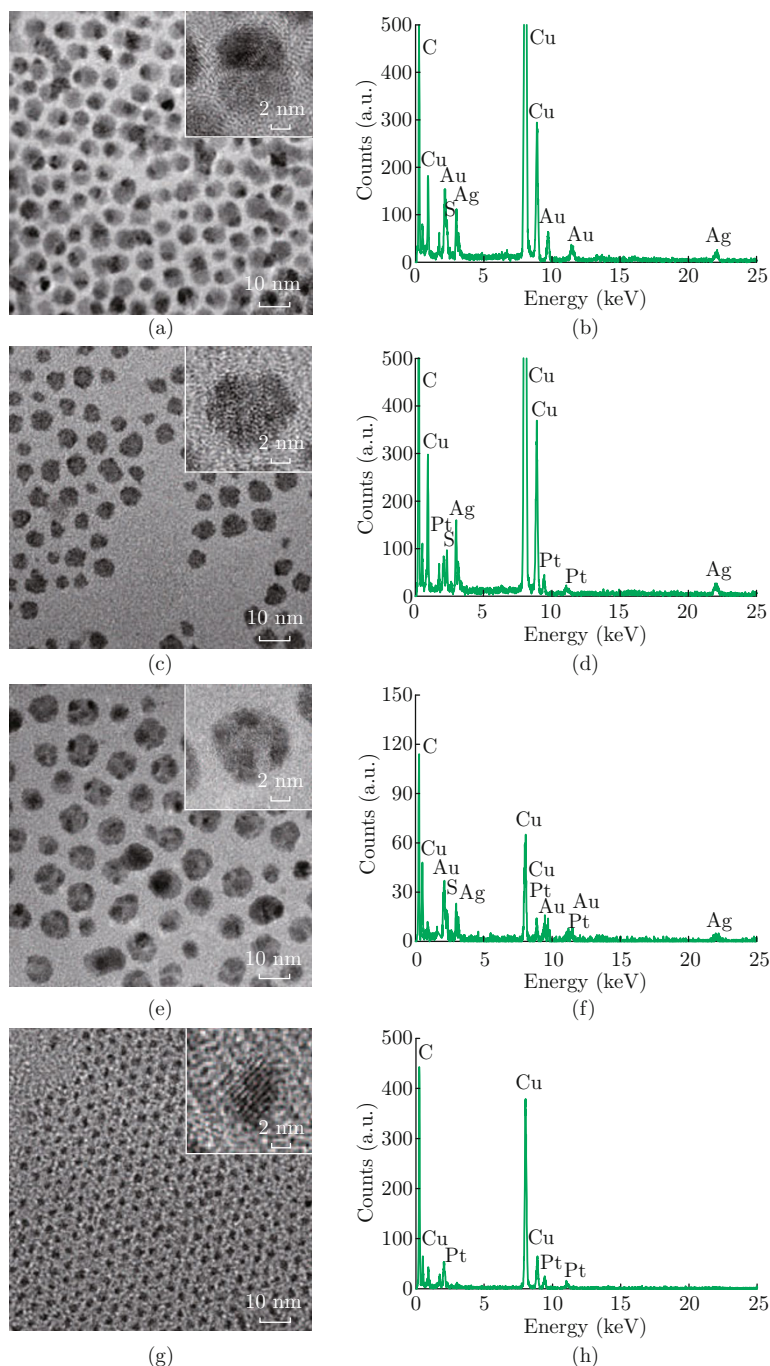


Fig. 3 TEM images (a,c,e,g) and corresponding EDX spectra (b,d,f,h) of Ag<sub>2</sub>S-Au (a,b), Ag<sub>2</sub>S-Pt (c,d), Ag<sub>2</sub>S-Au-Pt nanocomposites (e,f), and pure Pt nanoparticles (g,h). Insets are the HRTEM images of an individual particle.

analysis (Fig. 3(f)). Fig. 3(g) and 3(h) showed the TEM image and EDX analysis of the pure Pt nanoparticles derived from an ethanol mediated transfer method, which had analogous size (1.4 nm) to the Pt domains in the nanocomposites.

#### Electrochemical measurements of Pt-containing nanocomposites for oxidation of formic acid

The Ag<sub>2</sub>S-noble metal nanocomposites (Ag<sub>2</sub>S-Au, Ag<sub>2</sub>S-Pt, and Ag<sub>2</sub>S-Au-Pt) and pure Pt nanoparticles

were examined for their electrocatalytic activities for the formic acid oxidation reaction (FAOR) at room temperature. The voltammograms of formic acid oxidation in Fig. 4(a) were obtained in the potential window of 0-1 V at a scan rate of 20 mV s<sup>-1</sup>. The current densities in the voltammograms were normalized with the geometric area of the glassy carbon electrode. The peak current densities of these catalysts associated with formic acid oxidation in the forward and reverse scans were 70.2 mA cm<sup>-2</sup> and 193.1 mA cm<sup>-2</sup> for Pt,

167.7 mA cm<sup>-2</sup> and 300.4 mA cm<sup>-2</sup> for Ag<sub>2</sub>S-Pt, 225.3 mA cm<sup>-2</sup> and 427.6 mA cm<sup>-2</sup> for Ag<sub>2</sub>S-Au-Pt, respectively. The Ag<sub>2</sub>S-Au nanocomposites did not display catalytic activity for FAOR. The comparison in current densities indicated that the Ag<sub>2</sub>S-Au-Pt nanocomposites had higher activity for formic acid oxidation than that of Ag<sub>2</sub>S-Pt nanocomposites and pure Pt nanoparticles.

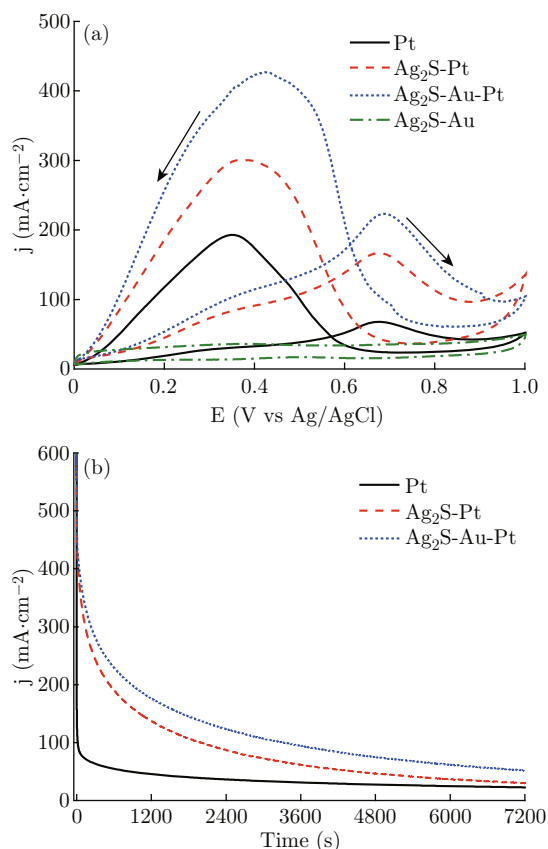


Fig. 4 Cyclic voltammograms of pure Pt nanoparticles and Pt-containing nanocomposites in argon-purged HClO<sub>4</sub> (0.1 M) with 1 M formic acid (a); and chronoamperograms of pure Pt nanoparticles and Pt-containing nanocomposites at 0.4 V vs. Ag/AgCl at room temperature in argon-purged HClO<sub>4</sub> (0.1 M) with 1 M formic acid (b).

Analogous to the superior catalytic activity of the Pt-containing nanocomposites for methanol oxidation [13], the enhanced catalytic activity of the Ag<sub>2</sub>S-Au-Pt nanocomposites for FAOR could also be attributed to the electronic coupling between the different domains in the nanocomposites. The XPS Pt 4f spectra of the Pt-containing nanocomposites (Ag<sub>2</sub>S-Pt, Ag<sub>2</sub>S-Au-Pt) and pure Pt nanoparticles were analyzed. As shown in Fig. 5, the Pt 4f spectra can be deconvoluted into two pairs of doublets, in which the more intense doublet (at 70.0 eV and 73.3 eV for pure Pt, 69.5 eV and 72.8 eV for Ag<sub>2</sub>S-Pt, 69.1 eV and 72.4 eV for Ag<sub>2</sub>S-Au-Pt) corresponded to Pt zero valent metal, while the second and weaker doublet, with binding energies of ~1.4

eV higher than those of Pt metal, could be assigned to Pt<sup>2+</sup> as in PtO and Pt(OH)<sub>2</sub> [19]. Compared with the Pt 4f<sub>7/2</sub> and 4f<sub>5/2</sub> binding energies of pure Pt nanoparticles, an appreciable shift to lower values was observed in the Ag<sub>2</sub>S-Pt and Ag<sub>2</sub>S-Au-Pt nanocomposites, suggesting that electrons were transferred to Pt from other domains of the nanocomposites. The comparison of the Pt 4f XPS spectra of Ag<sub>2</sub>S-Pt and Ag<sub>2</sub>S-Au-Pt nanocomposites further revealed that the presence of the Au domain could promote this electron-donating effect. This electron-donating effect to Pt domains might be induced by intra-particle charge transfer. Analogous charge transfer has been observed in the core-shell Au@PbS system, whereby the electrons transfer from PbS shell to the inner Au core resulted in the n-type to p-type change in hydrazine-treated PbS [20]. The electron flow from Au and Ag<sub>2</sub>S to the neighboring Pt domains due to the alignment of energy levels was believed to result in a substantial increase in the electron density around the Pt sites, which weakens the chemisorption of CO (a FAOR intermediate product and catalyst inhibitor) and hence promotes the FAOR. The long-term performance of pure Pt and Pt-containing Ag<sub>2</sub>S-metal nanocomposites in formic acid oxidation was illustrated in the chronoamperograms of Fig. 4(b). The slower rate of decay for the Pt-containing nanocomposites indicated their superior CO tolerance to the pure Pt catalysts.

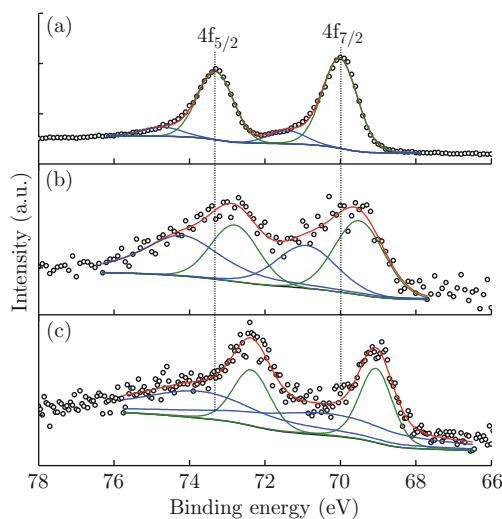


Fig. 5 4f XPS spectra of Pt in pure Pt nanoparticles (a); Ag<sub>2</sub>S-Pt (b); and Ag<sub>2</sub>S-Au-Pt nanocomposites (c).

## Conclusions

In summary, we have demonstrated an aqueous strategy for the synthesis of Pt-containing Ag<sub>2</sub>S-noble metal nanocomposites, which involved the preparation of Ag<sub>2</sub>S nanocrystals in aqueous phase, followed by the reaction or co-reduction of Au and Pt metal precursors.

sors with sodium citrate in aqueous phase. The Pt-containing nanocomposites displayed highly enhanced activity for catalyzing the formic acid oxidation reaction at room temperature due to the strong electronic coupling effect between the different domains in the nanocomposites. By optimizing the domain sizes for the nanocomposite system through varying the ratio of metal precursor to semiconductor seeds in the synthesis, further enhancement in FAOR activity could be expected.

## Acknowledgements

Financial support from the 100 Talents Program of the Chinese Academy of Sciences, National Natural Science Foundation of China (No.: 21173226, 21376247), and State Key Laboratory of Multiphase Complex Systems, Institute of Process Engineering, Chinese Academy of Sciences (MPCS-2011-D-08, MPCS-2010-C-02) is gratefully acknowledged.

## References

- [1] B. C. H. Steele and A. Heinzl, "Materials for fuel-cell technologies", *Nature* 414(6861), 345-352 (2001). <http://dx.doi.org/10.1038/35104620>
- [2] M. L. Perry and T. F. Fuller, "A historical perspective of fuel cell technology in the 20<sup>th</sup> century", *J. Electrochem. Soc.* 149(7), S59-S67 (2002). <http://dx.doi.org/10.1149/1.1488651>
- [3] X. Yu and P. G. Pickup, "Recent advances in direct formic acid fuel cells (DFAFC)", *J. Power Sources* 182(1), 124-132 (2008). <http://dx.doi.org/10.1016/j.jpowsour.2008.03.075>
- [4] R. Parsons and T. VanderNoot, "The oxidation of small organic molecules: A survey of recent fuel cell related research", *J. Electroanal. Chem. Interfacial Electrochem.* 257(1-2), 9-45 (1988). [http://dx.doi.org/10.1016/0022-0728\(88\)87028-1](http://dx.doi.org/10.1016/0022-0728(88)87028-1)
- [5] N. M. Marković and P. N. Ross, "Surface science studies of model fuel cell electrocatalysts", *Surf. Sci. Rep.* 45(4-6), 117-229 (2002). [http://dx.doi.org/10.1016/S0167-5729\(01\)00022-X](http://dx.doi.org/10.1016/S0167-5729(01)00022-X)
- [6] F. A. de Bruijn V. A. T. Dam and G. J. M. Janssen, "Review: durability and degradation issues of PEM fuel cell components", *Fuel Cells* 8(1), 3-22 (2008). <http://dx.doi.org/10.1002/face.200700053>
- [7] Y. Pan R. Zhang and S. L. Blair, "Anode poisoning study in direct formic acid fuel cells", *Electrochem. Solid-State Lett.* 12(3), B23-B26 (2009). <http://dx.doi.org/10.1149/1.3054278>
- [8] R. S. Jayashree J. S. Spendelow J. Yeom C. Rastogi M. A. Shannon and P. J. A. Kenis, "Characterization and application of electrodeposited Pt, Pt/Pd, and Pd catalyst structures for direct formic acid micro fuel cells", *Electrochim. Acta* 50(24), 4674-4682 (2005). <http://dx.doi.org/10.1016/j.electacta.2005.02.018>
- [9] J. B. Xu T. S. Zhao and Z. X. Liang, "Carbon supported platinum-gold alloy catalyst for direct formic acid fuel cells", *J. Power Sources* 185(2), 857-861 (2008). <http://dx.doi.org/10.1016/j.jpowsour.2008.09.039>
- [10] J. Chen B. Lim E. P. Lee and Y. Xia, "Shape-controlled synthesis of platinum nanocrystals for catalytic and electrocatalytic applications", *Nano Today* 4(1), 81-95 (2009). <http://dx.doi.org/10.1016/j.nantod.2008.09.002>
- [11] Z. Peng and H. Yang, "Designer platinum nanoparticles: Control of shape, composition in alloy, nanostructure and electrocatalytic property", *Nano Today* 4(2), 143-164 (2009). <http://dx.doi.org/10.1016/j.nantod.2008.10.010>
- [12] A. Chen and P. Holt-Hindle, "Platinum-based nanostructured materials: Synthesis, properties, and applications", *Chem. Rev.* 110(6), 3767-3804 (2010). <http://dx.doi.org/10.1021/cr9003902>
- [13] J. Yang and J. Y. Ying, "Nanocomposites of Ag<sub>2</sub>S and noble metals", *Angew. Chem. Int. Ed.* 50(20), 4637-4643 (2011). <http://dx.doi.org/10.1002/anie.201101213>
- [14] J. Yang X. Chen F. Ye C. Wang Y. Zheng and J. Yang, "Core-shell CdSe@Pt nanocomposites with superior electrocatalytic activity enhanced by lateral strain effect", *J. Mater. Chem.* 21(25), 9088-9094 (2011). <http://dx.doi.org/10.1039/C1JM11006C>
- [15] C. Rice S. Ha R. I. Masel P. Waszczuk A. Wieckowski and T. Barnard, "Direct formic acid fuel cells", *J. Power Sources* 111(1), 83-89 (2002). [http://dx.doi.org/10.1016/S0378-7753\(02\)00271-9](http://dx.doi.org/10.1016/S0378-7753(02)00271-9)
- [16] C. Rice S. Ha R. I. Masel and A. Wieckowski, "Catalysts for direct formic acid fuel cells", *J. Power Sources* 115(2), 229-235 (2003). [http://dx.doi.org/10.1016/S0378-7753\(03\)00026-0](http://dx.doi.org/10.1016/S0378-7753(03)00026-0)
- [17] Y. W. Rhee S. Y. Ha and R. I. Masel, "Crossover of formic acid through Nafion® membranes", *J. Power Sources* 117(1-2), 35-38 (2003). [http://dx.doi.org/10.1016/S0378-7753\(03\)00352-5](http://dx.doi.org/10.1016/S0378-7753(03)00352-5)
- [18] J. Yang E. H. Sargent S. O. Kelley and J. Y. Ying, "A general phase-transfer protocol for metal ions and its application in nanocrystal synthesis", *Nat. Mater.* 8(8), 683-689 (2009). <http://dx.doi.org/10.1038/nmat2490>
- [19] C. D. Wagner A. V. Naumkin A. Kraut-Vass J. W. Allison C. J. Powell and J. J. R. Rumble, NIST Standard Reference Database 20, Version 3.2 (Web Version).
- [20] J. S. Lee E. V. Shevchenko and D. V. Talapin, "Au-PbS core-shell nanocrystals: Plasmonic absorption enhancement and electrical doping *via* intra-particle charge transfer", *J. Am. Chem. Soc.* 130(30), 9673-9675 (2008). <http://dx.doi.org/10.1021/ja802890f>